Fault Detection and Severity Identification of Ball Bearings by Online Condition Monitoring

Article *in* IEEE Transactions on Industrial Electronics · December 2018

DOI: 10.1109/TIE.2018.2886789

6 authors, including:

Osama Abdeljaber
Linnaeus University
26 PUBLICATIONS **241** CITATIONS
SEE PROFILE

Sadok Sassi
Qatar University
32 PUBLICATIONS **307** CITATIONS
SEE PROFILE

Onur Avci
Qatar University
59 PUBLICATIONS **420** CITATIONS
SEE PROFILE

Serkan Kiranyaz
Qatar University
195 PUBLICATIONS **2,454** CITATIONS
SEE PROFILE

Fault Detection and Severity Identification of Ball Bearings by Online Condition Monitoring

Osama Abdeljaber, Sadok Sassi, Onur Avci, Serkan Kiranyaz, *Senior Member, IEEE,* Abdelrahman Ibrahim and Moncef Gabbouj, *Fellow Member, IEEE*

***Abstract*—The paper presents a fast, accurate and simple systematic approach for online condition monitoring and severity identification of ball bearings. This approach utilizes compact 1D convolutional neural networks (CNNs) to identify, quantify, and localize bearing damage. The proposed approach is verified experimentally under several single and multiple damage scenarios. The experimental results demonstrated that the proposed approach can achieve a high level of accuracy for damage detection, localization and quantification. Besides its real-time processing ability and superior robustness against the high-level noise presence, the compact and minimally-trained 1D CNNs in the core of the proposed approach can handle new damage scenarios with utmost accuracy.**

***Index Terms*—Ball bearings, damage detection, convolutional neural networks (CNNs), real-time monitoring.**

I. INTRODUCTION

OPERATIONAL efficiency and reliability of rotating machinery remain vital in modern applications as the technology gets more advanced and sophisticated in numerous industrial sectors. Rolling element bearings are common machine elements widely used in all types of rotating machines, from small hand-held devices to heavy-duty industrial systems. Serving as active interface between rotating components and stationary internal supports, bearings play a key role in the smooth functioning of the machine. However, due to their relatively low price, wide availability and operational ease, careless users tend to forget the "best-practices" in terms of maintenance, repair and handling. That is why more bearings continue to fail, causing possibly a catastrophic collapse of the machine and reducing the reliability and even availability of the entire production line.

Manuscript received May 4, 2018; revised Oct 23, 2018; accepted Nov 22, 2018.

O. Abdeljaber is with the Department of Civil and Architectural Engineering, Qatar University, Doha, Qatar (e-mail: o.abdeljaber@qu.edu.qa).

S. Sassi and A. Ibrahim are with the Department of Mechanical Engineering, Qatar University, Doha, Qatar (e-mail: sadok.sassi@qu.edu.qa, abdelrahman.saleh.18@gmail.com).

O. Avci is a former faculty member of the Department of Civil and Architectural Engineering, Qatar University, Doha, Qatar (e-mail: oavci@vt.edu).

S. Kiranyaz is with the Department of Electrical Engineering, Qatar University, Doha, Qatar (e-mail: mkiranyaz@qu.edu.qa).

M. Gabbouj is with the Department of Signal Processing, Tampere University of Technology, Tampere, Finland (e-mail: moncef.gabbouj@tut.fi).

Aging of bearings is inevitable since they are continuously exposed to short-term and long-term damage during operation. Early detection of embryonic bearing faults by real-time assessment of equipment condition using embedded sensors, allows replacement of the bearings, rather than larger parts of or the whole machine housing the bearing. Numerous studies have been published on condition monitoring, defect and fault detection; prognosis and diagnosis of bearings and their counterparts in rotating machinery. Different techniques, such as oil analysis, infrared thermography, acoustic emission, were used to track the degradation of bearings. These relatively easy techniques can pinpoint the existence of defects inside bearings but, unfortunately, they do not provide information about the location of the defect (e.g., the inner race, the outer race, the cage or the rolling element). Out of these approaches, vibration-based fault analysis appears to be the most efficient and advantageous in detecting, locating and quantifying bearing failure. Both time and frequency analysis have been used to investigate and track the effect of increasing defect sizes on the bearings' vibration response. In general, fault detection and severity identification algorithms can be categorized into model-based approaches and data-driven approaches. The model-based methods depend on a fundamental understanding of the physics of the process [1]. In data-driven methods, features can be extracted to characterize the historical process data as a priori knowledge to a diagnostic system. A large number of similar studies has utilized various tools and methods such as wavelet transforms [2], empirical mode decomposition method [3], fuzzy inference systems [4], Bayesian recursive framework [5], blind source separation [6], hidden Markov modeling [7], kernel-based neighborhood [8], probabilistic approaches [9], Welch method [10], regression-based methods [11], [12], and multivariate statistical analysis techniques such as kernel least squares based approach [13], and kernel direct decomposition-based method [14].

In addition to the methods above, machine learning based methods for fault diagnosis of bearings have recently been introduced. Such methods require extracting damage-sensitive features from the measured vibration signals and then training a classifier with the ability to analyze the extracted feature to assess the condition of the monitored bearing. For example, in the study by Samanta et al. [15], hand-crafted features such as mean, root mean square (RMS), and Kurtosis were extracted from the vibration signals of a rotating machine with normal and damaged bearings. After that, three different artificial neural network (ANN) models were trained to classify these features into undamaged or damaged states. Similarly, Patel and Upadhyay [16] used Kurtosis, RMS, and Crest factor as the features and then compared ANNs

and. Support Vector Machines (SVMs) in terms of classification performance. Also, Prieto et a. [17] used statistical time-features extracted from the vibration signals along with a hierarchical neural network classifier for damage diagnosis of bearings.

The main drawback of the aforementioned machine learning based methods is their strict dependence on the hand-crafted features used for classification of any vibration signal. Since the same features are to be used regardless of the vibration signal's characteristics, there is no guarantee that they will capture the discriminative properties of any vibration pattern and hence, training a classifier based on such sub-optimal features may eventually result in a poor classification performance [18].

Convolutional Neural Networks (CNNs) are known for their ability to fuse both feature extraction and classification into a single learning body and thus eliminate the need for such fixed and hand-crafted features [19]. Conventional deep CNNs (i.e. 2D CNNs) have been originally introduced to perform object recognition tasks for 2D signals such as images or videos. They have recently become the *de-facto* standard for many Computer Vision and Pattern Recognition tasks within large data archives as they achieved the state-of-the-art performances [20]–[22]. Recently, several researchers have attempted to use deep 2D CNNs for fault diagnosis of bearings [23]–[30]. Since they operate only on 2D data, they have used different techniques to represent the 1D vibration signals in 2D. The most commonly used technique is to directly reshape the vibration signal into an n×m matrix called "the vibration image" [28]. Another technique was used in [24] where two vibration signals were measured using two accelerometers. After that, Discrete Fourier Transform (DFT) was applied, and then the two transformed signals were concatenated into a matrix and used as an input to the 2D CNN. However, it is known that 2D CNNs, especially the ones with deep architectures, first of all, exhibit a high computational complexity. Hence, 2D CNNs may not be suitable for online fault detection when dealing with 1D signals without a special hardware. Moreover, proper training of deep CNNs requires large training sets in order to achieve a reasonable generalization capability. This usually requires a large-scale data augmentation of such limited vibration train data, which in turn further increases the computation complexity significantly.

To address these drawbacks, compact 1D CNNs have been recently developed to operate directly and more efficiently on 1D signals. They have displayed a fast and accurate performance in several real-time monitoring applications such as classification of electrocardiogram (ECG) beats [19], structural health monitoring [18], [31]–[33], and motor fault detection [34]. Additionally, two recent studies have utilized 1D CNNs for damage detection in bearings [35], [36]. In the first study [35], a 1D CNN was trained to classify the measured vibration signals into two classes, healthy or damaged. While this 1D CNN displayed a reasonable damage detection performance, it was not able to identify the location and severity of the detected bearing damage. In the second study conducted by Zhang et al. [36], both single and ensemble of deep 1D CNN(s) were created to detect, localize, and quantify bearing faults. The architecture of the deep 1D CNN used consisted of 6 large convolutional layers followed by two fully connected layers. The (ensemble of) deep network(s) was trained for a total of 10 specific damage cases representing the healthy state, three levels of ball damage, three levels of inner ring damages, and three levels of outer ring damages. Several "tricks" were used to improve the generalization performance of the deep CNN such as data augmentation, batch normalization, dropout, majority voting, and the use of ensemble of deep CNNs which achieved the best classification performance. The performance was tested for the 10 scenarios and under several noise levels to verify its robustness. Severe noise levels (e.g. 0dB or less) have proven to deteriorate the performance significantly. Besides its significant computational complexity, this method used more than 96% of the total data for training. Hence the assumption that such a large set of training data will be available may hinder the usage of this method in practice. Furthermore, the approach presented in [36] was only tested for single damage scenarios where in each scenario, a single defect was introduced to a particular bearing component. This is a crucial limitation because in real cases, the degradation pattern may manifest in an obvious increase of damage area, as well as multiple numbers and locations of defective elements. In particular, when the number of spalls in defective bearings [37] or the number of cracks in defective teeth gears [38] increases, some features which are recognized as highly sensitive to single damage scenarios, may lose their ability to track the internal degradation when the number of simultaneous defects increases.

In order to address the aforementioned drawbacks and limitations, in this study we propose a simpler, faster, and highly efficient and robust systematic approach for bearing damage monitoring (detection, localization and quantification). The significance and novel contributions of the proposed approach can be summarized as follows:

1) Rather than the deep counterparts, compact 1D CNNs used in the core of the proposed approach can accurately detect, localize, and quantify bearing damages in real-time even in noisy environments.
2) As a result of (1), the utilization of compact 1D CNNs will yield a high computational efficiency and achieve a high detection and localization performance with significantly limited training data. This will make the proposed solution more feasible in practical use, and more applicable for online fault detection without a special hardware setup that is required for deep CNNs (e.g., GPU farms or similar computing paradigms).
3) The proposed approach does not require any "tricks" to improve the classification performance, which makes the training simple and feasible using an ordinary computer.
4) Almost in all previous ML-based studies in the literature, such as [24], [36], the classifiers were trained and tested over the same, predefined set of damage scenarios and/or levels. Therefore, the proposed methods are only guaranteed to perform accurately when the condition of the monitored bearing matches one of the predefined states. The proposed approach does not make such a constraint on the working conditions.
5) In addition to the single bearing damage cases, the proposed fault diagnosis approach will be tested under multiple bearing damage scenarios in which several defects are introduced at the same time to the monitored bearing.

The rest of the paper is organized as follows. Section II presents an overview of the 1D CNNs and the main steps of the Back-Propagation training method. Section III presents the proposed systematic approach for bearing fault detection and localization. Section IV explains the experimental setup used in this work. The efficiency of proposed method is demonstrated with an extensive set of experiments in Section V. Finally, Section VI concludes the

This article has been accepted for publication in a future issue of this journal, but has not been fully edited. Content may change prior to final publication. Citation information: DOI 10.1109/TIE.2018.2886789, IEEE Transactions on Industrial Electronics

paper and suggests topics for future work.

II. 1D CNN Overview

The conventional 2D CNNs are a type of deep, biologically inspired feed-forward ANNs which are based on a core model for mammalian visual cortex. The proposed 1D CNNs [39] are their counterparts that work on 1D signals. Similar to 2D CNNs, two types of layers exist in the 1D CNNs: 1) the so-called "CNN-layers" where both 1D convolutions and sub-sampling occur, and 2) Fully-connected layers that are identical to the layers of a typical Multi-layer Perceptron (MLP) and hence called "MLP-layers".

CNNs perform (stacked) series of multi-scale sub-band decompositions in each hidden convolution-pooling layer. This ability gives CNN the opportunity to isolate the target pattern (may it be an object of any size, or an anomaly pattern in 1D signal) no matter the size and the time-frequency range it occupies [40]–[42]. A raw vibration signal can even defy a human expert inspector since it looks more like a white Gaussian noise rather than a well-structured signal with a proper pattern. When the signal is decomposed into many sub-bands in many scales, the CNN can then learn to "isolate" the signature of the anomaly (e.g. the bearing fault) from the common signature of the normal signal. The CNN-layers are basically the "fused" version of the convolutional and sub-sampling layers of the conventional 2D CNNs.

The structure of a 1D-CNN is determined by the following hyperparameters, which are usually determined by trial-and-error:

1) Number of hidden CNN-layers.
2) Number of hidden fully-connected layers.
3) Number of neurons in each CNN and fully-connected layer.
4) Filter kernels size.
5) Subsampling factor.

Three consecutive CNN layers of a 1D CNNs are shown in Fig. 1. In this sample illustration, the 1D filter kernels have size 3 and the sub-sampling factor is 2 where the k^{th} neuron in the hidden CNN layer, l, first performs a sequence of convolutions, the sum of which is passed through the activation function, f, followed by the sub-sampling operation. This is basically the predominant difference between 1D and 2D CNNs, where 1D arrays replace 2D matrices for both kernels and feature maps. At the end, the CNN layers process the raw 1D data and "learn to extract" such features that can be used in the classification task performed by the MLP-layers. Therefore, both feature extraction and classification operations are *fused* into one process that can be optimized to maximize the classification performance. This is the main advantage of the 1D CNNs that can also provide a low computational complexity since the only costly operation is a sequence of 1D convolutions that are nothing but linear weighted sums of two 1D arrays. Such a linear operation during both forward and back-propagation can be executed efficiently in parallel.

Since the learning stage is tuned for bearing damage detection in this study, a 1D CNN structure can now blend the extraction of features and "damage learning" stages of the raw accelerometer data from wireless sensors. As such, the CNN topology will permit the variations in the input layer dimension since the sub-sampling factor of the output CNN layer is set adaptively [39]. Details regarding forward and back-propagation in CNN layers are covered in Appendix A.

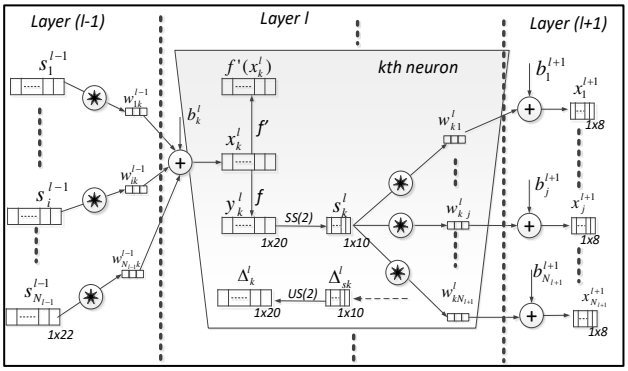

Fig. 1. Three consecutive hidden CNN layers of a 1D CNN.

III. The Proposed System

The proposed approach requires training two individual 1D CNNs. The first CNN, CNN_i is responsible of evaluating the condition of the inner ring, while the second one, CNN_o monitors the condition of the outer ring. The input to both CNNs is the vibration signal measured by the accelerometers. The output of CNN_i is used to extract an index p_i that represents the likelihood of damage at the inner ring, while the output of CNN_o is used to compute p_o which represent the likelihood of damage at the outer ring. Both CNNs are completely independent, which means that they can operate in a decentralized manner to produce p_i and p_o.

A. Training phase

This is an offline operation (performed once) that trains two independent 1D CNNs. The first step is to produce three sets of data required to train each 1D CNN, as follows:

1) The first dataset $\mathbf{C}_1$ consists of vibration signals corresponding to the undamaged case.
2) The second dataset $\mathbf{C}_2$ consists of vibration signals corresponding to a severe inner ring defect.
3) The third dataset $\mathbf{C}_3$ consists of vibration signals corresponding to a severe outer ring defect.

It is important to note that unlike the previous CNN-based bearing fault detection methods in [35], [36] which require the corresponding set of data for each damage level to train the classifier(s), the proposed method requires signals only from the severe inner- and outer-ring damage scenarios. The choice of the defect size in the severe inner and outer ring damage scenarios is up to the designer. This decision will determine the sensitivity of the proposed fault detection method to inner and outer ring defects. The next step is to divide these signals into a number of non-overlapping frames, each with a fixed length of n_s samples:

$$\mathbf{C}_1 = [\mathbf{C}_{1,1} \quad \mathbf{C}_{1,2} \quad \cdots \quad \mathbf{C}_{1,N_1}] \tag{1}$$

$$\mathbf{C}_2 = [\mathbf{C}_{2,1} \quad \mathbf{C}_{2,2} \quad \cdots \quad \mathbf{C}_{2,N_2}] \tag{2}$$

$$\mathbf{C}_3 = [\mathbf{C}_{3,1} \quad \mathbf{C}_{3,2} \quad \cdots \quad \mathbf{C}_{3,N_3}] \tag{3}$$

where N_1, N_2, and N_3 denote the number of frames in $\mathbf{C}_1$, $\mathbf{C}_2$, and $\mathbf{C}_3$, respectively. Frames in, $\mathbf{C}_1$, $\mathbf{C}_2$, and $\mathbf{C}_3$ are then grouped as follows:

$$\mathbf{U}_i = [\mathbf{C}_{1,1} \quad \mathbf{C}_{1,2} \quad \cdots \quad \mathbf{C}_{1,N_1} \quad \mathbf{C}_{3,1} \quad \mathbf{C}_{3,2} \quad \cdots \quad \mathbf{C}_{3,N_3}] \tag{4}$$

$$\mathbf{D}_i = [\mathbf{C}_{2,1} \quad \mathbf{C}_{2,2} \quad \cdots \quad \mathbf{C}_{2,N_2}] \tag{5}$$

$$\mathbf{U}_o = [\mathbf{C}_{1,1} \quad \mathbf{C}_{1,2} \quad \cdots \quad \mathbf{C}_{1,N_1} \quad \mathbf{C}_{2,1} \quad \mathbf{C}_{2,2} \quad \cdots \quad \mathbf{C}_{2,N_2}] \tag{6}$$

$$\mathbf{D}_o = [\mathbf{C}_{3,1} \quad \mathbf{C}_{3,2} \quad \cdots \quad \mathbf{C}_{3,N_3}] \tag{7}$$

where $\mathbf{U}_i$ contains the frames measured while the inner ring is undamaged and $\mathbf{D}_i$ denotes the frames measured while the inner ring is damaged. Similarly, $\mathbf{U}_o$ represents the frames measured

while the outer ring is undamaged and $\mathbf{D}_o$ denotes the frames measured while the outer ring is damaged. Next, the frames in each of the sets $\mathbf{U}_i$, $\mathbf{D}_i$, $\mathbf{U}_o$, and $\mathbf{D}_o$ are normalized between -1 and 1 and then randomly shuffled for training efficiency. The resulting normalized and shuffled vectors can be represented as:

$$\mathbf{UN}_i = [\mathbf{UN}_{i,1} \quad \mathbf{UN}_{i,2} \quad \cdots \quad \mathbf{UN}_{i,N_1+N_3}] \tag{8}$$
$$\mathbf{DN}_i = [\mathbf{DN}_{i,1} \quad \mathbf{DN}_{i,2} \quad \cdots \quad \mathbf{DN}_{i,N_2}] \tag{9}$$
$$\mathbf{UN}_o = [\mathbf{UN}_{i,1} \quad \mathbf{UN}_{i,2} \quad \cdots \quad \mathbf{UN}_{i,N_1+N_2}] \tag{10}$$
$$\mathbf{DN}_o = [\mathbf{DN}_{i,1} \quad \mathbf{DN}_{i,2} \quad \cdots \quad \mathbf{DN}_{i,N_3}] \tag{11}$$

The normalized and shuffled frames in $\mathbf{UN}_i$ and $\mathbf{DN}_i$ are then used to train the first classifier, CNN_i which is responsible for the damage monitoring (detection and quantification) in the inner ring. This classifier should be able to process any input frame and determine whether it is corresponding to an undamaged or a severely damaged inner ring. Likewise, normalized and shuffled frames in $\mathbf{UN}_o$ and $\mathbf{DN}_o$ are used to train the second classifier, CNN_o which is responsible for the damage monitoring in the outer ring. It is worth noting here that with a proper training, CNN_i will eventually learn to ignore defects in the outer ring since the frames corresponding to severe outer ring damage are placed in $\mathbf{UN}_i$. Similarly, CNN_o will ignore the defects caused by severe inner ring damages since $\mathbf{UN}_o$ contains samples from a vibration signal generated under a severe inner ring defect. The training of CNN_i and CNN_o is conducted according to the back-propagation methodology explained in Section II. Fig. 2 illustrates the proposed CNN training process.

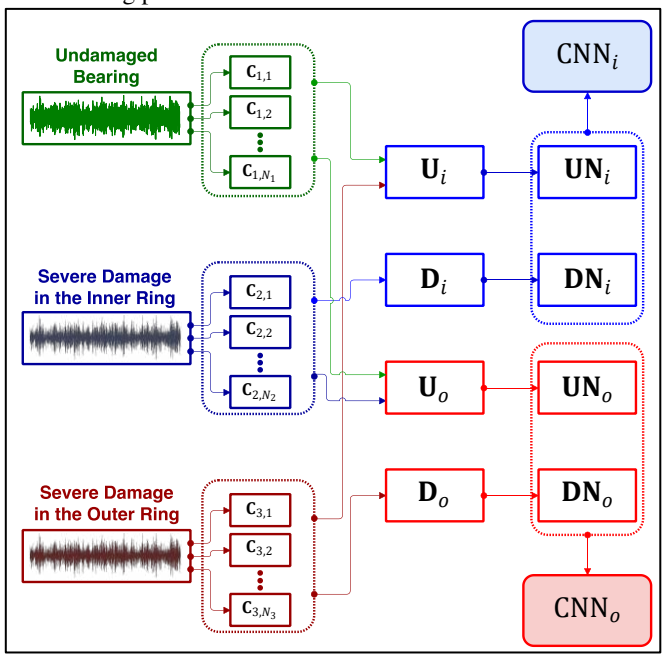

Fig. 2. Training of the two 1D CNNs, CNN_i and CNN_o.

B. Damage monitoring

Once the training phase is completed, CNN_i will be able to classify any input frame to one of the following classes:

- Class 1: Undamaged inner ring.
- Class 2: Severe defect in the inner ring.

Similarly, CNN_o will classify the input frame to one of the following classes:

- Class 3: Undamaged outer ring.
- Class 4: Severe defect in the outer ring.

As illustrated in Fig. 3, the two classifiers can be used to assess the condition of the bearing according to the following procedure:

1) Measure the vibration response of the bearing. The measured signal is denoted as $\mathbf{M}$.
2) Divide the measured signal $\mathbf{M}$ into N_T non-overlapping frames, each with a fixed length n_s samples:
$$\mathbf{M} = [\mathbf{M}_1 \quad \mathbf{M}_2 \quad \cdots \quad \mathbf{M}_{N_T}] \tag{12}$$
3) Normalize the amplitude of each frame between -1 and 1:
$$\mathbf{MN} = [\mathbf{MN}_1 \quad \mathbf{MN}_2 \quad \cdots \quad \mathbf{MN}_{N_T}] \tag{13}$$
4) Feed the normalized frames in $\mathbf{MN}$ to both CNN_i and CNN_o classifiers.
5) Classifier CNN_i will assign each of the N_T measured frames either to Class 1 (undamaged inner ring) or to Class 2 (severe damage in the inner ring). Similarly, classifier CNN_o will assign each of the N_T measured frames either to Class 3 (undamaged outer ring) or to Class 3 (severe damage in the outer ring).
6) Assuming that N_i is the number of frames assigned by CNN_i to Class 2 and N_o is the number of frames classified by CNN_o to Class 4, it is possible to express the following probabilities:
$$P_i = \frac{N_i}{N_T}; \qquad P_o = \frac{N_o}{N_T} \tag{14}$$
where P_i is the probability that a severe defect exists in the inner ring, and P_o is the probability that a severe defect exists in the outer ring.

It is expected that an undamaged bearing will result in very low values of P_i and P_o (close to zero). Also, it is anticipated that P_i will increase gradually as the size/severity of the defect in the inner ring increases, while P_o will not be affected. Similarly, P_o is likely to increase as the size of the defect in the outer ring increases, while P_i remains unchanged. Therefore, both P_i and P_o can be used to detect, localize and quantify any bearing damage.

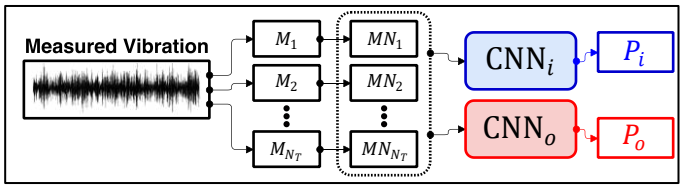

Fig. 3. Quantification and localization of bearing damage using CNN_i and CNN_o.

IV. Experimental Setup

To measure the vibration generated by a damaged bearing, under several running conditions of load and speed, a test rig was carefully designed and accurately manufactured. This test rig will be used to support the bearing, to rotate it at a required speed and to subject it to the preset load. Since this testing machine will be used in many experiments, the test rig system is designed to take into consideration the ease of replacing the bearing for each test run. This device is a "Machinery Fault Simulator" (a modified version of the original simulator built by Spectra Quest Inc.) (Fig. 4). Several parts of the original machine were removed and replaced with new ones. Because mounting and dismounting bearings are delicate operations, time-consuming and may permanently damage the bearing or the shaft, an innovative solution based on elastically expandable geometry was adopted at the right end of the shaft to fit this purpose. The vibration signal was collected using an ICP accelerometer (PCB Piezotronics, Model No. 352C33, 100mV/g). The readings were controlled by a four-channel NI-9234 sound and vibration input module at a

This article has been accepted for publication in a future issue of this journal, but has not been fully edited. Content may change prior to final publication. Citation information: DOI 10.1109/TIE.2018.2886789, IEEE Transactions on Industrial Electronics

sampling frequency of 51.2 kHz during time intervals of 10 seconds each.

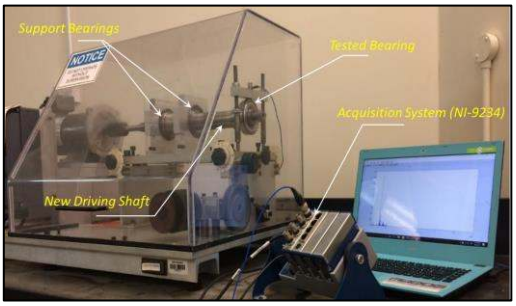

Fig. 4. The experimental setup.

To simplify defects seeding process on the raceways, a sufficiently large tested bearing was selected. For this purpose, a bore diameter of 40 mm was chosen (bearing type NSK-6208). In general, a bearing can contain both localized and distributed defects. Condition monitoring and system maintenance basically rely on vibration signals caused by localized defects, while signals resulting from distributed defects are used in quality assurance monitoring. This study focuses on localized defects only. Such defects were brought to the bearings using Electric Discharge Machining (Fig. 5).

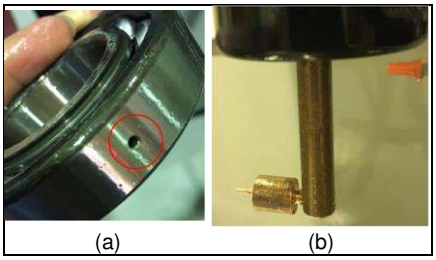

Fig. 5. Bearing defects machining. (a) A sample of defect seeded on the outer race. (b) Example of the machining tool.

V. EXPERIMENTAL RESULTS

With the aforementioned experimental setup, vibration signals corresponding to the following 27 scenarios were acquired:

1) Reference case: 3 scenarios corresponding to 3 similar undamaged bearings.
2) Damage in the inner ring: 9 scenarios corresponding to 9 levels of damage in the inner ring: 0.35, 0.40, 0.50, 0.58, 1.00, 1.50, 2.00, 2.50, and 3.00 mm.
3) Damage in the outer ring: 9 scenarios corresponding to 9 levels of damage in the outer ring: 0.35, 0.40, 0.50, 0.58, 1.00, 1.50, 2.00, 2.50, and 3.00 mm.
4) 6 scenarios corresponding to the following multiple damage cases:
   a. 0.50 mm inner defect + 2.00 mm outer defect.
   b. 2.00 mm inner defect + 2.00 mm outer defect.
   c. Three inner defects: 1.00+2.00+3.00 mm.
   d. 2.00 mm inner defect + 0.50 mm outer defect.
   e. 1.00 mm inner defect + 1.00 mm outer defect.
   f. Three outer defects: 1.00+2.00+3.00 mm.

Examples of the defects introduced to the bearings are provided in Fig. 6. For each of the 27 scenarios, 10 vibration signals were measured. Each signal is 10 secs long and sampled at 51.2 kHz. All signals were filtered by a lowpass filter with a cutoff frequency of 6400 Hz, then down-sampled to 12800 Hz, and divided into frames with a fixed length $n_s = 1024$ samples.

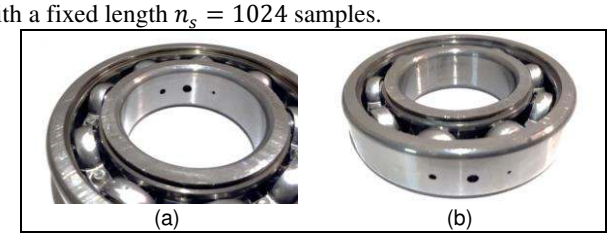

Fig. 6. Examples of multiple defects introduced to the bearings. (a) Defects on inner raceway. (b) Defects on outer raceway.

A. Training of CNN_i and CNN_o

The aforementioned data sets were used to train and evaluate classifiers CNN_i and CNN_o as explained in Section III. In this demonstration, defects in inner and outer rings which are larger than or equal to 2.50 mm, which represent a defect-to-ball ratio of 21%, were considered as "severe" defects. Hence, the sets, $\mathbf{C}_1$, $\mathbf{C}_2$, and $\mathbf{C}_3$ required to train the classifiers CNN_i and CNN_o were defined as follows:

1) Set $\mathbf{C}_1$ contains 5 signals out of the 3×10=30 signals available for the reference case. Note that these 5 signals correspond to the first undamaged bearing. The remaining 5 signals of the first undamaged bearing along with the 10+10=20 signals of the second and third undamaged bearings were kept for evaluating the CNNs.
2) Set $\mathbf{C}_2$ contains 5 out of the 10 available signals acquired at 2.50 mm inner ring damage along with 5 out of the 10 available signals acquired at 3.00 mm inner ring damage.
3) Set $\mathbf{C}_3$ contains 5 out of the 10 available signals acquired at 2.50 mm outer ring damage along with 5 out of the 10 available signals acquired at 3.00 mm outer ring damage.

One can notice here that 7 sets of signals corresponding to 0.35 up to 2.00 mm defects in both inner and outer rings along with the signals under the multiple damage cases were not used for training. Next, the signals in the three sets were divided into frames having a fixed length of n_s = 1024 samples. Then, the frames in $\mathbf{C}_1$, $\mathbf{C}_2$, and $\mathbf{C}_3$ were grouped, normalized, and shuffled as explained in Section III.A. Accordingly, each of the resulting $\mathbf{UN}_i$ and $\mathbf{UN}_o$ contained (5+5+5)×12800 Hz×10 sec/1024=1875 frames, while each of $\mathbf{DN}_i$ and $\mathbf{DN}_o$ contained (5+5)×12800 Hz×10 sec/1024=1250 frames. 90% of the frames in $\mathbf{UN}_i$ and $\mathbf{DN}_i$ were used to train the classifier CNN_i and 90% of the frames in $\mathbf{UN}_o$ and $\mathbf{DN}_o$ were used to train CNN_o. The remaining 10% was left out for validation. A compact CNN architecture was used for both classifiers with only two hidden convolution layers and two fully-connected layers. Classifiers CNN_i and CNN_o had only (3, 3) neurons in the two hidden convolution layers and (10, 10) neurons in the two MLP-layers. The kernel size and subsampling factor were set to 40 and 20, respectively. The following stopping criteria for BP training was considered:

1) The train classification error (CE) of 1%.
2) Maximum 200 BP iterations.

The CNNs were trained according to the back-propagation methodology detailed in Section II. For CNN_i the classification error was 0.53% for the training set and 0.64% for the testing set, while for CNN_o, the classification error was 0.00% for both training and testing sets. Achieving such accuracy levels above 99% for the test sets can be considered an elegant damage monitoring performance level for the proposed solution.

This article has been accepted for publication in a future issue of this journal, but has not been fully edited. Content may change prior to final publication. Citation information: DOI 10.1109/TIE.2018.2886789, IEEE Transactions on Industrial Electronics

B. Performance evaluations

The damage monitoring (detection, localization, and quantification) performance was evaluated over all the scenarios presented earlier. The signals used for the training phase (listed in Section V.A) were totally excluded from this evaluation. For each scenario, all signals under that scenario (except the ones using for CNN training) were decimated as explained in Section V and then divided into frames with a fixed length of 1024 samples. The frames were then normalized and fed to both CNN_i and CNN_o. According to the classification output of the two classifiers, the indices P_i and P_o were computed.

For the three undamaged scenarios corresponding to three similar undamaged bearings, P_i and P_o values were both correctly assigned as zero indicating that both the inner and outer rings are undamaged. As shown in Fig. 7a, for the scenarios associated with a single defect in the inner ring, the resulting P_i values are proportional to the size (severity) of the defect, while zero P_o values were obtained across all damage levels indicating that the outer ring is undamaged. For small defects (0.35 to 0.58 mm), the P_i values ranged between 0 to 0.066 which indicate an insignificant inner ring damage. For medium-sized defects in the inner ring (1.00 to 2.00 mm), the P_i values vary between 0.37 to 0.76, while for severe defects (2.50 and 3.00 mm) the resulting P_i values were close to 1.00. In a similar fashion, as displayed in Fig. 7b, for the damage scenarios associated with a single defect in the outer ring, the P_o values are well-correlated with the defect size and the P_i values are all zeros. The fact that the classifiers were able to handle small and medium-sized defects in inner and outer rings is quite interesting indeed since both CNN_i and CNN_o were trained using only signals from undamaged and severely damaged scenarios. This demonstrates an elegant interpolation ability of the CNNs trained according to the proposed systematic approach to deal with such damage cases that are completely new (unseen). In reality, this is a desired and practical property that voids the need for creating all damage scenarios for a proper damage monitoring.

In addition to the single defect cases, the proposed method was further tested over the six multiple damage scenarios. As shown in Fig. 7c, the resulting P_i and P_o values are both in agreement with the size of the defects. For all six cases, the classifiers were able to correctly quantify the damage in at least one of the damaged components. Again, this highlights the ability of the proposed approach to deal with entirely new scenarios which were not used in CNN training.

C. Effect of the total number of frames N_T

As mentioned in Section III.B, in order to evaluate the condition of the monitored bearing, the vibration signal is measured for a certain amount of time and then divided into N_T frames. The N_T frames are then processed by the two CNNs to compute N_i and N_o, which can be used to calculate the probabilities of damage P_i and P_o as explained by Equation (25). It is clear from the equation that the probabilities are dependent on the total number of frames N_T. Therefore, a sufficient number of frames should be provided to the classifiers in order to achieve an acceptable degree of accuracy.

The effect of N_T was investigated for 4 damage cases which are: 1) 1.50 mm inner ring defect, 2) 3.00 mm inner ring defect, 3) 1.00 mm outer ring defect, and 4) 3.00 mm outer ring defect. For each case, the corresponding vibration signal was fed into the classifier in a frame-by-frame manner. As shown in Fig. 8, starting from $N_T = 4$ frames, the probabilities P_i and P_o were computed for every N_T value up until $N_T = 100$ frames. The results for the 4 damage cases suggest that P_i and P_o stabilize starting at $N_T = 13$ frames. Hence, a signal consisting of 13 frames (equivalent to 13×1024/12800 = 1.04 sec) is sufficient for accurately characterize the condition of the bearing.

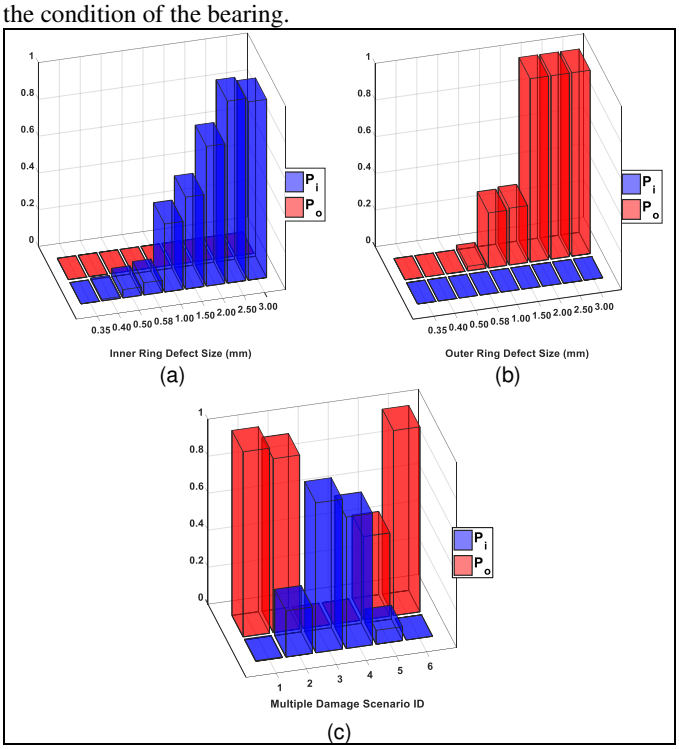

Fig. 7. P_i and P_o values obtained by the proposed CNN-based approach for (a) nine levels of inner ring damage, (b) nine levels of outer ring damage, and (c) six multiple damage scenarios.

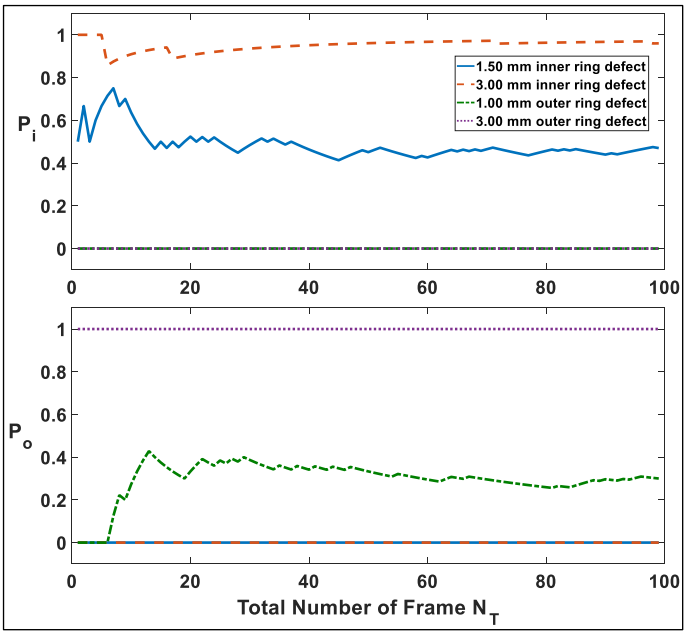

Fig. 8. P_i and P_o values obtained for 4 damage scenarios with N_T values ranging from 4 to 100.

D. Robustness against noise

In order to test the robustness of the proposed system against the measurement noise, the signals corresponding to all scenarios (except the ones used for CNN training) are contaminated by

This article has been accepted for publication in a future issue of this journal, but has not been fully edited. Content may change prior to final publication. Citation information: DOI 10.1109/TIE.2018.2886789, IEEE Transactions on Industrial Electronics

different levels of additive noise. The level of noise is typically measured by the signal-to-noise ratio (SNR) expressed as,

$$\text{SNR} = 10\log_{10}\left(\frac{P_{\text{signal}}}{P_{\text{noise}}}\right) \quad (15)$$

where P_{signal} is the power of the signal and P_{noise} is the power of the White Gaussian noise.

The results for the undamaged cases, single inner ring defect scenarios, single outer ring defect scenarios, and multiple defects scenarios are shown in Table 1, Fig. 9, Fig. 10, and Fig. 11, respectively. It is clear from the results that both CNN_i and CNN_o displayed a robust performance in terms of damage localization and quantification even at SNR values as low as -2dB. This is another crucial advantage of the proposed approach compared to the state-of-the-art method in [36], the performance of which suffered significantly with the increasing noise power, especially at SNR values around 2dB and lower.

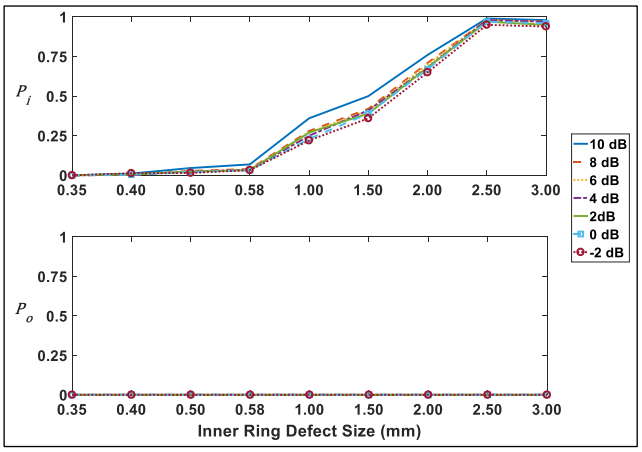

Fig. 9. P_i and P_o values for the 9 damage levels in the inner ring under different noise levels.

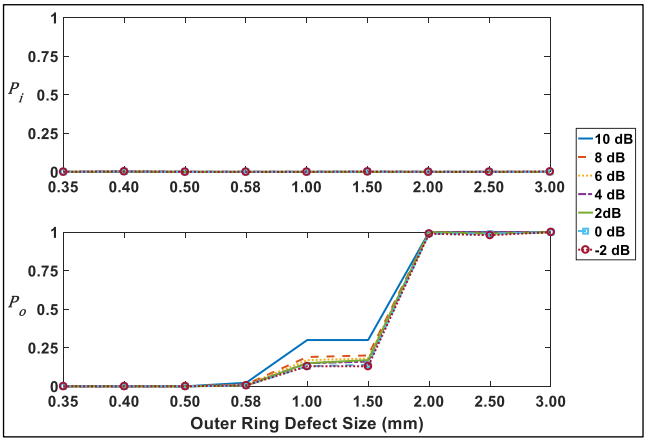

Fig. 10. P_i and P_o values for the 9 damage levels in the outer ring under different noise levels.

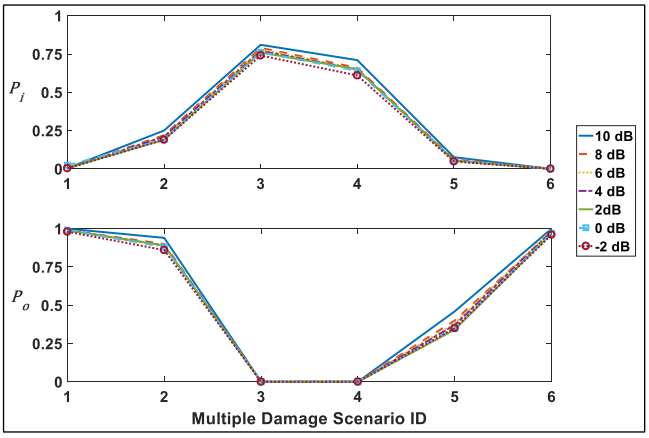

Fig. 11. P_i and P_o values for the 6 multiple damage scenarios under different noise levels.

TABLE I

P_i AND P_o VALUES OBTAINED BY THE PROPOSED CNN-BASED APPROACH FOR THREE UNDAMAGED SCENARIOS UNDER DIFFERENT NOISE LEVELS.

ID	SNR = 10 dB		SNR = 8 dB		SNR = 6 dB		SNR = 4 dB		SNR = 2 dB		SNR = 0 dB		SNR = -2 dB	
	P_i	P_o	P_i	P_o	P_i	P_o	P_i	P_o	P_i	P_o	P_i	P_o	P_i	P_o
1	0	0	0	0	0	0	0	0	0.0016	0	0	0	0	0
2	0	0	0.0016	0	0	0	0.004	0	0	0	0.0024	0	0.0016	0
3	0.0032	0	0.0048	0	0.0032	0	0.0016	0	0.008	0	0.004	0	0.0016	0

TABLE II

COMPARISON WITH THE PREVIOUS 1D-CNN BASED METHODS.

	Eren [35]	Zhang et al. [36]	Current work
Damage detection	Yes	Yes	Yes
Damage quantification	No	Yes	Yes
Damage localization	No	Yes	Yes
Number of defects	Single defect	Single defect	Single and multiple defects
Data required for training	Undamaged + all damaged cases	Undamaged + all damaged cases	Undamaged + a single severely damaged case
1D-CNN architecture	Medium-sized 1D-CNN	An ensemble of deep networks	Shallow 1D-CNN.
Tricks required for training	None	Data augmentation, batch normalization, dropout, and majority voting	None
Robustness against noise	Not investigated	Performance deterioration at 0 dB (or less) noise levels.	Robust even at noise levels as low as -2dB

E. Complexity analysis

The proposed system is implemented using MATLAB [43] and C++ by MS Visual Studio 2013 in 64-bit. Since the compact 1D CNNs are used, this is a non-GPU implementation; however, Intel ® OpenMP API is used to obtain multiprocessing with a shared memory. This program is capable of carrying out the forward and back-propagation steps required for training and using the CNNs. The MATLAB [43] codes are then developed and utilized: 1) to extract raw signal arrays, U_i, D_i, U_o, D_o based on the methodology detailed in Section III.A, 2) to compute the indices P_i and P_o directly from the raw vibration signals using the trained CNN_i and CNN_o as explained in Section III.B, and 3) to present the final output in a proper GUI with the corresponding probability plots/graphs The experimental verification was conducted using a computer with I7-4910MQ at 2.9 GHz (8 cores) and 32-Gb memory.

As mentioned earlier, the key feature of the proposed 1D CNN-based damage detection technique is that the computational time and power required to classify the signals are significantly reduced due to the fact that shallow 1D CNN architectures are used. To demonstrate this feature, CNN_i was used to classify a 2-sec vibration signal having a sampling frequency of 12800 Hz (i.e. the signal consists of 25600 samples). The signal was divided to 25 frames each having $n_s = 1024$ samples. The total time required for the classification of this 2-sec signal was only 240 msec. This speed is about 8× faster than the real-time requirement. The same speed was obtained for CNN_o as well since CNN_o has exactly the same architecture as CNN_i.

F. Comparison with previous 1D-CNN based methods

To highlight its significance, the method proposed in the current paper is compared with the previous 1D-CNN based methods developed by Eren [35] and Zhang et al. [36] as shown in Table II.

VI. Conclusions

This paper proposes a novel online bearing monitoring system for detection, quantification, and localization of bearing defects. The core of the system is composed of two compact 1D CNNs that can fuse the feature extraction and classification processes of a traditional damage monitoring system into a single learning body. In this way, the computational burden and the problems that arise due to the choice and design of hand-crafted features are avoided and features can be optimized to maximize the detection/quantification performance. The experimental results demonstrate that the aforementioned five objectives are all achieved, and the following novel contributions are accomplished:

1) The proposed systematic approach is able to accurately localize and quantify bearing damage. The values of the indices P_i and P_o assigned by the proposed approach is well-correlated with the actual amount of damage introduced to the components of the monitored bearing.
2) The minimally-trained classifiers, CNN_i and CNN_o are able to handle all new (unseen) damage scenarios with utmost accuracy.
3) The proposed system displayed a superior robustness against the severe additive noise.
4) The utilization of the compact 1D CNNs in the core of the proposed system voids the need for large training data, special hardware and many compulsory tricks such as data augmentation, batch normalization, dropout, majority voting, etc.
5) As a result, with these crucial properties, the proposed system can conveniently be used in practice for online health monitoring of bearings. It will be further interesting to test it over the new motors with unseen bearings without any training ever performed. This will be the topic of our future work.
6) In this work, the two 1D CNNs (corresponding to the inner and outer rings) were trained and tested under the same speed and torque conditions. The results showed that CNNs with a very shallow structure were able to achieve the required accuracy level. This shallow structure allows very fast training performance. Therefore, it is feasible to train an individual set of 1D-CNNs for each possible level of speed and torque. Nevertheless, it would be quite interesting to investigate if a 1D-CNN trained under a specific level of speed and torque will perform properly under another set of conditions. This can be also a subject for future work.

APPENDIX

A. Forward and back-propagation in CNN-layers

In the CNN-layers, one-dimensional forward propagation (1D-FP) is defined as:

$$x_k^l = b_k^l + \sum_{i=1}^{N_{l-1}} \mathrm{conv1D}\left(w_{ik}^{l-1}, s_i^{l-1}\right) \tag{16}$$

where x_k^l is defined as the input, b_k^l is defined as the bias of the k^{th} neuron at layer l, s_i^{l-1} is the output of the i^{th} neuron at layer $l-1$, w_{ik}^{l-1} is the kernel from the i^{th} neuron at layer $l-1$ to the k^{th} neuron at layer l. The output y_k^l can be written from the input x_k^l as,

$$y_k^l = f(x_k^l) \quad \text{and} \quad s_k^l = y_k^l \downarrow ss \tag{17}$$

where s_k^l stands for the output of the neuron and $\downarrow ss$ represents the down-sampling operation with factor, ss.

The back-propagation (BP) methodology can be summarized as follows. The BP of the error starts from the output MLP-layer. Assume $l = 1$ for the input layer and $l = L$ for the output layer. Let N_L be the number of classes in the database; then, for an input vector p, and its target and output vectors, t_i^p and $\left[y_1^L, \cdots, y_{N_L}^L\right]$, respectively. With that, in the output layer for the input p; the mean-squared error (MSE), E_p, can be expressed as follows:

$$E_p = \mathrm{MSE}\left(t_i^p, \left[y_1^L, \cdots, y_{N_L}^L\right]\right) = \sum_{i=1}^{N_L} \left(y_i^L - t_i^p\right)^2 \tag{18}$$

To find the derivative of E_p by each network parameter, the delta error, $\Delta_k^l = \frac{\partial E}{\partial x_k^l}$ should be computed. Specifically, for updating the bias of that neuron and all weights of the neurons in the preceding layer, one can use the chain-rule of derivatives as,

$$\frac{\partial E}{\partial w_{ik}^{l-1}} = \Delta_k^l y_i^{l-1} \quad \text{and} \quad \frac{\partial E}{\partial b_k^l} = \Delta_k^l \tag{19}$$

Then, the BP of the delta-error from the next layer (l+1) to layer l is expressed as:

$$\frac{\partial E}{\partial s_k^l} = \Delta s_k^l = \sum_{i=1}^{N_{l+1}} \frac{\partial E}{\partial x_i^{l+1}} \frac{\partial x_i^{l+1}}{\partial s_k^l} = \sum_{i=1}^{N_{l+1}} \Delta_i^{l+1} w_{ki}^l \tag{20}$$

Following BP to the input delta, Δ_k^l, as,

$$\Delta_k^l = \frac{\partial E}{\partial y_k^l}\frac{\partial y_k^l}{\partial x_k^l} = \frac{\partial E}{\partial \mathrm{us}_k^l}\frac{\partial \mathrm{us}_k^l}{\partial y_k^l} f'(x_k^l) = \mathrm{up}(\Delta s_k^l)\beta\, f'(x_k^l) \quad (21)$$

where $\beta = (ss)^{-1}$. Then, the BP of the delta error $\left(\Delta s_k^l \overset{\Sigma}{\leftarrow} \Delta_l^{l+1}\right)$ can be expressed as:

$$\Delta s_k^l = \sum_{i=1}^{N_{l+1}} \mathrm{conv\ 1Dz}\left(\Delta_l^{l+1}, \mathrm{rev}(w_{ki}^l)\right) \quad (22)$$

where $\mathrm{rev}(.)$ is used to reverse the array and $\mathrm{conv\ 1Dz}(.,.)$ is used to perform full convolution in 1D. This is another crucial difference from 2D CNNs where the 2D matrix operations such as lateral rotation (*rot180*) and 2D convolution (*conv2D*) are replaced by *reverse* (rev) and 1D convolution (*conv1D and conv1Dz)* operations [18], [34]. As such, the weight and bias sensitivities can be expressed as follows:

$$\frac{\partial E}{\partial w_{ik}^l} = \mathrm{conv\ 1D}(s_k^l, \Delta_l^{l+1}) \quad \text{and} \quad \frac{\partial E}{\partial b_k^l} = \sum_n \Delta_k^l(n) \quad (23)$$

Once the weight and bias sensitivities are computed, they can then be used to update biases and weights with the learning factor, ε as,

$$w_{ik}^{l-1}(t+1) = w_{ik}^{l-1}(t) - \varepsilon \frac{\partial E}{\partial w_{ik}^{l-1}} \quad (24)$$

$$b_k^l(t+1) = b_k^l(t) - \varepsilon \frac{\partial E}{\partial b_k^l} \quad (25)$$

Further details of the BP algorithm are given in [18], [34].

REFERENCES

[1] S. Sassi, B. Badri, and M. Thomas, "A numerical model to predict damaged bearing vibrations," *JVC/Journal of Vibration and Control*, vol. 13, no. 11, pp. 1603–1628, 2007.

[2] L. Eren and M. J. Devaney, "Bearing Damage Detection via Wavelet Packet Decomposition of the Stator Current," *IEEE Transactions on Instrumentation and Measurement*, vol. 53, no. 2, pp. 431–436, 2004.

[3] J. Ben Ali, N. Fnaiech, L. Saidi, B. Chebel-Morello, and F. Fnaiech, "Application of empirical mode decomposition and artificial neural network for automatic bearing fault diagnosis based on vibration signals," *Applied Acoustics*, vol. 89. pp. 16–27, 2015.

[4] B. Satish and N. D. R. Sarma, "A fuzzy BP approach for diagnosis and prognosis of bearing faults in induction motors," *IEEE Power Engineering Society General Meeting 2005*, pp. 1–4, 2005.

[5] Z. Mao and M. D. Todd, "A Bayesian recursive framework for ball-bearing damage classification in rotating machinery," *Structural Health Monitoring*, vol. 15, no. 6, pp. 668–684, 2016.

[6] M. J. Roan, J. G. Erling, and L. H. Sibul, "A new, non-linear, adaptive, blind source separation approach to gear tooth failure detection and analysis," *Mechanical Systems and Signal Processing*, vol. 16, no. 5, pp. 719–740, 2002.

[7] H. Ocak and K. a. Loparo, "A new bearing fault detection and diagnosis scheme based on hidden Markov modeling of vibration signals," *IEEE International Conference on Acoustics, Speech, and Signal Processing. Proceedings (Cat. No.01CH37221)*, vol. 5, pp. 3141–3144, 2001.

[8] V. Sugumaran, G. R. Sabareesh, and K. I. Ramachandran, "Fault diagnostics of roller bearing using kernel based neighborhood score multi-class support vector machine," *Expert Systems with Applications*, vol. 34, no. 4, pp. 3090–3098, 2008.

[9] B. Zhang, C. Sconyers, C. Byington, R. Patrick, M. E. Orchard, and G. Vachtsevanos, "A Probabilistic Fault Detection Approach: Application to Bearing Fault Detection," *IEEE Transactions on Industrial Electronics*, vol. 58, no. 5, pp. 2011–2018, 2011.

[10] M. Pacas, S. Villwock, and R. Dietrich, "Bearing damage detection in permanent magnet synchronous machines," *2009 IEEE Energy Conversion Congress and Exposition*, pp. 1098–1103, 2009.

[11] M. Schlechtingen and I. Ferreira Santos, "Comparative analysis of neural network and regression based condition monitoring approaches for wind turbine fault detection," *Mechanical Systems and Signal Processing*, vol. 25, no. 5. pp. 1849–1875, 2011.

[12] R. K. Upadhyay, L. A. Kumaraswamidhas, and M. S. Azam, "Rolling element bearing failure analysis: A case study," *Case Studies in Engineering Failure Analysis*, vol. 1, no. 1, pp. 15–17, 2013.

[13] G. Wang and J. Jiao, "A Kernel Least Squares Based Approach for Nonlinear Quality-Related Fault Detection," *IEEE Transactions on Industrial Electronics*, vol. 64, no. 4, pp. 3195–3204, 2017.

[14] G. Wang, J. Jiao, and S. Yin, "A kernel direct decomposition-based monitoring approach for nonlinear quality-related fault detection," *IEEE Transactions on Industrial Informatics*, vol. 13, no. 4, pp. 1565–1574, 2017.

[15] B. Samanta, K. R. Al-Balushi, S. A. Al-Araimi, and S. Katagiri, "Bearing Fault Detection Using Artificial Neural Networks and Genetic Algorithm," *EURASIP Journal on Applied Signal Processing*, vol. 3, pp. 366–377, 2004.

[16] J. P. Patel and S. H. Upadhyay, "Comparison between Artificial Neural Network and Support Vector Method for a Fault Diagnostics in Rolling Element Bearings," *Procedia Engineering*, vol. 144, pp. 390–397, 2016.

[17] M. D. Prieto, G. Cirrincione, A. G. Espinosa, J. A. Ortega, and H. Henao, "Bearing fault detection by a novel condition-monitoring scheme based on statistical-time features and neural networks," *IEEE Transactions on Industrial Electronics*, vol. 60, no. 8, pp. 3398–3407, 2013.

[18] O. Abdeljaber, O. Avci, S. Kiranyaz, M. Gabbouj, and D. J. Inman, "Real-time vibration-based structural damage detection using one-dimensional convolutional neural networks," *Journal of Sound and Vibration*, vol. 388, pp. 154–170, Feb. 2017.

[19] S. Kiranyaz, T. Ince, and M. Gabbouj, "Personalized Monitoring and Advance Warning System for Cardiac Arrhythmias," *Scientific Reports*, vol. 7, no. 1, 2017.

[20] D. C. Cire\csan, U. Meier, L. M. Gambardella, and J. Schmidhuber, "Deep, Big, Simple Neural Nets for Handwritten Digit Recognition," *Neural Comput.*, vol. 22, no. 12, pp. 3207–3220, Dec. 2010.

[21] D. Scherer, A. Müller, and S. Behnke, "Evaluation of Pooling Operations in Convolutional Architectures for Object Recognition," in *Proceedings of the 20th International Conference on Artificial Neural Networks: Part III*, 2010, pp. 92–101.

[22] S. Kiranyaz, M. A. Waris, I. Ahmad, R. Hamila, and M. Gabbouj, "Face segmentation in thumbnail images by data-adaptive convolutional segmentation networks," *2016 IEEE International Conference on Image Processing (ICIP)*. pp. 2306–2310, 2016.

[23] X. Guo, L. Chen, and C. Shen, "Hierarchical adaptive deep convolution neural network and its application to bearing fault diagnosis," *Measurement: Journal of the International Measurement Confederation*, vol. 93, pp. 490–502, 2016.

[24] O. Janssens, V. Slavkovikj, B. Vervisch, K. Stockman, M. Loccufier, S. Verstockt, R. Van de Walle, and S. Van Hoecke, "Convolutional Neural Network Based Fault Detection for Rotating Machinery," *Journal of Sound and Vibration*, vol. 377, pp. 331–345, 2016.

[25] D.-T. Hoang and H.-J. Kang, "Convolutional Neural Network Based Bearing Fault Diagnosis," in *Intelligent Computing Theories and Application*, 2017, pp. 105–111.

[26] Zhang, Wei, Peng, Gaoliang, and Li, Chuanhao, "Bearings Fault Diagnosis Based on Convolutional Neural Networks with 2-D Representation of Vibration Signals as Input," *MATEC Web Conf.*, vol. 95, p. 13001, 2017.

[27] D. K. Appana, W. Ahmad, and J.-M. Kim, "Speed Invariant Bearing Fault Characterization Using Convolutional Neural Networks," pp. 189–198, 2017.

[28] Z. Wei, P. Gaoliang, and L. Chuanhao, "Bearings Fault Diagnosis Based on Convolutional Neural Networks with 2- D Representation of Vibration Signals as Input," vol. 13001, pp. 1–5, 2017.

[29] S. Li, G. Liu, X. Tang, J. Lu, and J. Hu, "An Ensemble Deep Convolutional Neural Network Model with Improved D-S Evidence Fusion for Bearing Fault Diagnosis," *Sensors*, vol. 17, no. 8, p. 1729, 2017.

[30] K. B. Lee, S. Cheon, C. O. Kim, L. Dalfino, F. Puntillo, A. Mosca, R. Monno, M. Luigia, S. Coppolecchia, G. Miragliotta, F. Bruno, D. Verstraete, M. Engineering, M. Engineering, M. F. Guo, X. D. Zeng, D. Y. Chen, and N. C. Yang, "An adaptive deep convolutional neural network for rolling bearing fault diagnosis," *Hindawi Shock and Vibration*, vol. 30, no. 99, pp. 1–29, 2017.

[31] O. Avci, O. Abdeljaber, S. Kiranyaz, and D. Inman, "Structural Damage Detection in Real Time: Implementation of 1D Convolutional Neural Networks for SHM Applications," in *Structural Health Monitoring & Damage Detection, Volume 7: Proceedings of the 35th IMAC, A Conference and Exposition on Structural Dynamics 2017*, C. Niezrecki, Ed. Cham: Springer International Publishing, 2017, pp. 49–54.

[32] O. Abdeljaber, O. Avci, M. S. Kiranyaz, B. Boashash, H. Sodano, and D.

J. Inman, "1-D CNNs for structural damage detection: Verification on a structural health monitoring benchmark data," *Neurocomputing*, 2017.

[33] O. Avci, O. Abdeljaber, S. Kiranyaz, M. Hussein, and D. J. Inman, "Wireless and Real-Time Structural Damage Detection: A Novel Decentralized Method for Wireless Sensor Networks," *Journal of Sound and Vibration*, 2018.

[34] T. Ince, S. Kiranyaz, L. Eren, M. Askar, and M. Gabbouj, "Real-Time Motor Fault Detection by 1-D Convolutional Neural Networks," *IEEE Transactions on Industrial Electronics*, vol. 63, no. 11. pp. 7067–7075, 2016.

[35] L. Eren, "Bearing fault detection by one-dimensional convolutional neural networks," *Mathematical Problems in Engineering*, vol. 2017, 2017.

[36] W. Zhang, C. Li, G. Peng, Y. Chen, and Z. Zhang, "A deep convolutional neural network with new training methods for bearing fault diagnosis under noisy environment and different working load," *Mechanical Systems and Signal Processing*, vol. 100, pp. 439–453, 2018.

[37] S. Sassi, B. Badri, and M. Thomas, "Tracking surface degradation of ball bearings by means of new time domain scalar indicators," *International Journal of COMADEM*, vol. 11, no. 3, pp. 36–45, 2008.

[38] A. Mohamed, S. Sassi, and M. R. Paurobally, "Model-based analysis of gears' dynamic behavior in the presence of multiple cracks," *Journal of Shock and Vibration*, 2018.

[39] S. Kiranyaz, T. Ince, R. Hamila, and M. Gabbouj, "Convolutional Neural Networks for patient-specific ECG classification," in *Proceedings of the Annual International Conference of the IEEE Engineering in Medicine and Biology Society, EMBS*, 2015.

[40] S. Mallat and S. Zhong, "Characterization of Signals From Multiscale Edges," *IEEE Transactions on Pattern Analysis and Machine Intelligence*, vol. 14, no. 7, pp. 710–732, 1992.

[41] A. Krizhevsky, "Learning Multiple Layers of Features from Tiny Images," 2009.

[42] M. D. Zeiler and R. Fergus, "Visualizing and understanding convolutional networks," *Lecture Notes in Computer Science (including subseries Lecture Notes in Artificial Intelligence and Lecture Notes in Bioinformatics)*, vol. 8689 LNCS, no. PART 1, pp. 818–833, 2014.

[43] The Mathworks Inc., "MATLAB - MathWorks," *www.mathworks.com/products/matlab*, 2016.

Osama Abdeljaber was born in Kuwait, 1989. He received his BS degree in Civil Engineering at Kuwait University (2011). He received his MS (2014) degree in Structural Engineering at Jordan University of Science and Technology, Irbid, Jordan. He joined Qatar University as a Research Assistant and PhD student in 2014. His research interests are structural dynamics, structural health monitoring and vibration control.

Sadok Sassi is a professor in mechanical engineering at Qatar University. He has a Ph.D. in mechanical engineering from "École Polytechique de Montréal". He is also an active member of the Canadian Machinery Vibration Association. His research interests are in vibration analysis and predictive maintenance of rotating machines. He had previously acquired a wide industrial experience as the group leader at the "Sound and Vibration" cluster at QU. He is the supervisor of the master student Abdelrahman Aly.

Onur Avci was born in Turkey, 1979. He received his BS degree in Civil Engineering at Middle East Technical University (2000), Ankara, Turkey. He received his MS (2002) and PhD (2005) degrees in Civil Engineering at Virginia Tech, Blacksburg, VA. He later worked in structural engineering firms in the United States such as Walter P Moore Associates (2005-2006); Weidlinger Associates (2006-2010) and AECOM (2010-2012) where he designed more than 4 million square feet of structural space. He joined Qatar University as an Assistant Professor in 2012 and left in 2017. His research interests are structural dynamics, structural health monitoring and structural steel. He is a licensed professional engineer in the States of Connecticut and New York.

Serkan Kiranyaz (SM'13) is a Professor in Qatar University, Doha, Qatar. He published 2 books, 5 book chapters, more than 50 journal papers in high impact journals, and more than 100 papers in international conferences. Prof. Kiranyaz has co-authored the papers which have nominated or received the "Best Paper Award" in ICIP 2013, ICPR 2014, ICIP 2015 and IEEE TSP 2018. He had the most-popular articles in the years 2010 and 2016, and most-cited article in 2018 in IEEE Transactions on Biomedical Engineering. During 2010-2015 he authored the 4th most-cited article of the Neural Networks journal. His research team has won the 2nd and 1st places in PhysioNet Grand Challenges 2016 and 2017, among 48 and 75 international teams, respectively.

Abdelrahman Ibrahim is a graduate student at Qatar University. He is involved in the field of vibration signal analysis and condition monitoring of damaged bearings.

Moncef Gabbouj (F'11) is a well-established world expert in the field of image processing, and held the prestigious post of Academy of Finland Professor during 2011-2015. He has been leading the Multimedia Research Group for nearly 25 years and managed successfully a large number of projects in excess of 18M Euro. He has supervised 45 PhD theses and over 50 MSc theses. He is the author of several books and over 700 papers. His research interests include Big Data analytics, multimedia content-based analysis, indexing and retrieval, artificial intelligence, machine learning, pattern recognition, nonlinear signal and image processing and analysis, voice conversion, and video processing and coding. Dr. Gabbouj is a Fellow of the IEEE and member of the Academia Europaea and the Finnish Academy of Science and Letters. He is the past Chairman of the IEEE CAS TC on DSP and committee member of the IEEE Fourier Award for Signal Processing. He served as associate editor and guest editor of many IEEE, and international journals.